

Conditional simulation of max-stable processes

BY C. DOMBRY, F. ÉYI-MINKO,

Laboratoire de Mathématiques et Application, Université de Poitiers, Téléport 2, BP 30179,

F-86962 Futuroscope-Chasseneuil cedex, France

clement.dombry@math.univ-poitiers.fr, frederic.eyi.minko@math.univ-poitiers.fr

AND M. RIBATET

Department of Mathematics, Université Montpellier 2, 4 place Eugène Bataillon, 34095 cedex

2 Montpellier, France

mathieu.ribatet@math.univ-montp2.fr

SUMMARY

Since many environmental processes such as heat waves or precipitation are spatial in extent, it is likely that a single extreme event affects several locations and the areal modelling of extremes is therefore essential if the spatial dependence of extremes has to be appropriately taken into account. This paper proposes a framework for conditional simulations of max-stable processes and give closed forms for Brown–Resnick and Schlather processes. We test the method on simulated data and give an application to extreme rainfall around Zurich and extreme temperature in Switzerland. Results show that the proposed framework provides accurate conditional simulations and can handle real-sized problems.

Some key words: Conditional simulation; Markov chain Monte Carlo; Max-stable process; Precipitation; Regular conditional distribution; Temperature.

1. INTRODUCTION

Max-stable processes arise naturally when studying extremes of stochastic processes and therefore play a major role in the statistical modelling of spatial extremes (Buishand et al, 2008; Padoan et al., 2010; Davison et al., 2011). Although a different spectral characterization of max-stable processes exists (de Haan, 1984), for our purposes the most useful representation is (Schlather, 2002)

$$Z(x) = \max_{i \geq 1} \zeta_i Y_i(x), \quad x \in \mathbb{R}^d, \quad (1)$$

where $\{\zeta_i\}_{i \geq 1}$ are the points of a Poisson process on $(0, \infty)$ with intensity $d\Lambda(\zeta) = \zeta^{-2}d\zeta$ and Y_i are independent replicates of a non-negative continuous sample path stochastic process Y such that $E\{Y(x)\} = 1$ for all $x \in \mathbb{R}^d$. It is well known that Z is a max-stable process on \mathbb{R}^d with unit Fréchet margins (de Haan & Ferreira, 2006; Schlather, 2002). Although (1) takes the pointwise maximum over an infinite number of points $\{\zeta_i\}$ and processes Y_i , it is possible to get approximate realizations from Z (Schlather, 2002; Oesting et al., 2011).

Based on (1) several parametric max-stable models have been proposed (Schlather, 2002; Brown & Resnick, 1977; Kabluchko et al., 2009; Davison et al., 2011) and share the same finite dimensional distribution functions

$$\text{pr}\{Z(x_1) \leq z_1, \dots, Z(x_k) \leq z_k\} = \exp \left[-E \left\{ \max_{j=1, \dots, k} \frac{Y(x_j)}{z_j} \right\} \right],$$

where $k \in \mathbb{N}$, $z_1, \dots, z_k > 0$ and $x_1, \dots, x_k \in \mathbb{R}^d$.

Apart from the Smith model (Genton et al., 2011), only the bivariate cumulative distribution functions are explicitly known. To bypass this hurdle, de Haan & Pereira (2006) propose a semi-parametric estimator and Padoan et al. (2010) suggest the use of the maximum pairwise likelihood estimator.

97 Paralleling the use of the variogram in classical geostatistics, the extremal coefficient function
 98 (Schlather & Tawn, 2003; Cooley et al., 2006)

$$100 \theta(x_1 - x_2) = -z \log \text{pr}\{Z(x_1) \leq z, Z(x_2) \leq z\}$$

101
 102 is widely used to summarize the spatial dependence of extremes. It takes values in the interval
 103 $[1, 2]$; the lower bound indicates complete dependence, and the upper one independence.

104 The last decade has seen many advances to develop a geostatistic of extremes and software is
 105 available to practitioners (Wang, 2010; Schlather, 2011; Ribatet, 2011). However an important
 106 tool currently missing is conditional simulation of max-stable processes. In classical geostatistic
 107 based on Gaussian models, conditional simulations are well established (Chilès & Delfiner,
 108 1999) and provide a framework to assess the distribution of a Gaussian random field given val-
 109 ues observed at fixed locations. For example, conditional simulations of Gaussian processes have
 110 been used to model land topography (Mandelbrot, 1982).

111 Conditional simulation of max-stable processes is a long-standing problem (Davis & Resnick,
 112 1989, 1993). Wang & Stoev (2011) provide a first solution, but their framework is limited to
 113 processes having a discrete spectral measure and thus may be too restrictive to appropriately
 114 model the spatial dependence in complex situations.

115 Based on the recent developments on the regular conditional distribution of max-infinitely
 116 divisible processes, the aim of this paper is to provide a methodology to get conditional sim-
 117 ulations of max-stable processes with continuous spectral measures. More formally for a study
 118 region $\mathcal{X} \subset \mathbb{R}^d$, our goal is to derive an algorithm to sample from the regular conditional distribu-
 119 tion of $Z \mid \{Z(x_1) = z_1, \dots, Z(x_k) = z_k\}$ for some $z_1, \dots, z_k > 0$ and k conditioning locations
 120 $x_1, \dots, x_k \in \mathcal{X}$.

121

122

123

2. CONDITIONAL SIMULATION OF MAX-STABLE PROCESSES

2.1. General framework

This section reviews some key results of an unpublished paper available from the first author with a particular emphasis on max-stable processes. Our goal is to give a more practical interpretation of their results from a simulation perspective. To this aim, we recall two key results and propose a procedure to get conditional realizations of max-stable processes.

Let $\mathbb{R}^{\mathcal{X}}$ be the space of on $\mathcal{X} \subset \mathbb{R}^d$ and let $\Phi = \{\varphi_i\}_{i \geq 1}$ be a Poisson point process on $\mathbb{R}^{\mathcal{X}}$ where $\varphi_i(x) = \zeta_i Y_i(x)$ ($i = 1, 2, \dots$) with ζ_i and Y_i as in (1). We write $f(x) = \{f(x_1), \dots, f(x_k)\}$ for all random functions $f: \mathcal{X} \rightarrow \mathbb{R}$ and $x = (x_1, \dots, x_k) \in \mathcal{X}^k$. It is not difficult to show that for all Borel set $A \subset \mathbb{R}^k$, the Poisson point process $\{\varphi_i(x)\}_{i \geq 1}$ defined on \mathbb{R}^k has intensity measure

$$\Lambda_x(A) = \int_0^\infty \text{pr} \{ \zeta Y(x) \in A \} \zeta^{-2} d\zeta.$$

The point process Φ is called regular if the intensity measure Λ_x has an intensity function λ_x , i.e., $\Lambda_x(dz) = \lambda_x(z) dz$, for all $x \in \mathcal{X}^k$.

The first key point is that provided the point process Φ is regular, the intensity function λ_x and the conditional intensity function

$$\lambda_{s|x,z}(u) = \frac{\lambda_{(s,x)}(u,z)}{\lambda_x(z)}, \quad (s,x) \in \mathcal{X}^{m+k}, \quad u \in \mathbb{R}^m, \quad z \in (0, +\infty)^k, \quad (2)$$

drives how the conditioning terms $\{Z(x_j) = z_j\}$ ($j = 1, \dots, k$) are met.

The second key point is that, conditionally on $Z(x) = z$, the Poisson point process Φ can be decomposed into two independent point processes, say $\Phi = \Phi^- \cup \Phi^+$, where

$$\Phi^- = \{\varphi \in \Phi: \varphi(x_i) < z_i \text{ for all } i = 1, \dots, k\},$$

$$\Phi^+ = \{\varphi \in \Phi: \varphi(x_i) = z_i \text{ for some } i = 1, \dots, k\}.$$

193 Before introducing a procedure to get conditional realizations of max-stable processes, we
 194 introduce notation and make connections with the pioneering work of Wang & Stoev (2011).

195 A function $\varphi \in \Phi^+$ such that $\varphi(x_i) = z_i$ for some $i \in \{1, \dots, k\}$ is called an extremal func-
 196 tion associated to x_i and denoted by $\varphi_{x_i}^+$. It is easy to show that there exists almost surely a
 197 unique extremal function associated to x_i . Although $\Phi^+ = \{\varphi_{x_1}^+, \dots, \varphi_{x_k}^+\}$ almost surely, it
 198 might happen that a single extremal function contributes to the random vector $Z(x)$ at sev-
 199 eral locations x_i , e.g., $\varphi_{x_1}^+ = \varphi_{x_2}^+$. To take such repetitions into account, we define a random
 200 partition $\theta = (\theta_1, \dots, \theta_\ell)$ of the set $\{x_1, \dots, x_k\}$ into $\ell = |\theta|$ blocks and extremal functions
 201 $(\varphi_1^+, \dots, \varphi_\ell^+)$ such that $\Phi^+ = \{\varphi_1^+, \dots, \varphi_\ell^+\}$ and $\varphi_j^+(x_i) = z_i$ if $x_i \in \theta_j$ and $\varphi_j^+(x_i) < z_i$ if
 202 $x_i \notin \theta_j$ ($i = 1, \dots, k; j = 1, \dots, \ell$). Wang & Stoev (2011) call the partition θ the hitting sce-
 203 nario. The set of all possible partitions of $\{x_1, \dots, x_k\}$, denoted \mathcal{P}_k , identifies all possible hitting
 204 scenarios.

205 From a simulation perspective, the fact that Φ^- and Φ^+ are independent given $Z(x) = z$
 206 is especially convenient and suggests a three-step procedure to sample from the conditional
 207 distribution of Z given $Z(x) = z$.

208 **THEOREM 1.** *Suppose that the point process Φ is regular and let $(x, s) \in \mathcal{X}^{k+m}$. For $\tau =$
 209 $(\tau_1, \dots, \tau_\ell) \in \mathcal{P}_k$ and $j = 1, \dots, \ell$, define $I_j = \{i: x_i \in \tau_j\}$, $x_{\tau_j} = (x_i)_{i \in I_j}$, $z_{\tau_j} = (z_i)_{i \in I_j}$,
 210 $x_{\tau_j^c} = (x_i)_{i \notin I_j}$ and $z_{\tau_j^c} = (z_i)_{i \notin I_j}$. Consider the three-step procedure:*

211 *Step 1.* Draw a random partition $\theta \in \mathcal{P}_k$ with distribution

212
 213
$$\pi_x(z, \tau) = \text{pr} \{ \theta = \tau \mid Z(x) = z \} = \frac{1}{C(x, z)} \prod_{j=1}^{|\tau|} \lambda_{x_{\tau_j}}(z_{\tau_j}) \int_{\{u_j < z_{\tau_j^c}\}} \lambda_{x_{\tau_j^c} | x_{\tau_j}, z_{\tau_j}}(u_j) \mathrm{d}u_j,$$

214 where the normalization constant is

215
 216
$$C(x, z) = \sum_{\tilde{\tau} \in \mathcal{P}_k} \prod_{j=1}^{|\tilde{\tau}|} \lambda_{x_{\tilde{\tau}_j}}(z_{\theta_j}) \int_{\{u_j < z_{\tilde{\tau}_j^c}\}} \lambda_{x_{\tilde{\tau}_j^c} | x_{\tilde{\tau}_j}, z_{\tilde{\tau}_j}}(u_j) \mathrm{d}u_j.$$

217
 218
 219

241 *Step 2.* Given $\tau = (\tau_1, \dots, \tau_\ell)$, draw ℓ independent random vectors $\varphi_1^+(s), \dots, \varphi_\ell^+(s)$ from
 242 the distribution

$$243 \quad \text{pr} \left\{ \varphi_j^+(s) \in dv \mid Z(x) = z, \theta = \tau \right\} = \frac{1}{C_j} \left\{ \int \mathbf{1}_{\{u < z_{\tau_j^c}\}} \lambda_{(s, x_{\tau_j^c}) | x_{\tau_j}, z_{\tau_j}}(v, u) du \right\} dv$$

244

where $\mathbf{1}_{\{\cdot\}}$ is the indicator function and

245

$$246 \quad C_j = \int \mathbf{1}_{\{u < z_{\tau_j^c}\}} \lambda_{(s, x_{\tau_j^c}) | x_{\tau_j}, z_{\tau_j}}(v, u) dudv,$$

247 and define the random vector $Z^+(s) = \max_{j=1, \dots, \ell} \varphi_j^+(s)$.

248

Step 3. Independently draw a Poisson point process $\{\zeta_i\}_{i \geq 1}$ on $(0, \infty)$ with intensity $\zeta^{-2} d\zeta$
 249 and $\{Y_i\}_{i \geq 1}$ independent copies of Y , and define the random vector

250

$$251 \quad Z^-(s) = \max_{i \geq 1} \zeta_i Y_i(s) \mathbf{1}_{\{\zeta_i Y_i(x) < z\}}.$$

252

Then the random vector $\tilde{Z}(s) = \max\{Z^+(s), Z^-(s)\}$ follows the conditional distribution of
 253 $Z(s)$ given $Z(x) = z$.

254 The corresponding conditional cumulative distribution function is

$$255 \quad \text{pr} \{Z(s) \leq a \mid Z(x) = z\} = \frac{\text{pr}\{Z(s) \leq a, Z(x) \leq z\}}{\text{pr}\{Z(x) \leq z\}} \sum_{\tau \in \mathcal{P}_k} \pi_x(z, \tau) \prod_{j=1}^{|\tau|} F_{\tau, j}(a), \quad (3)$$

256

where

257

$$258 \quad F_{\tau, j}(a) = \text{pr} \left\{ \varphi_j^+(s) \leq a \mid Z(x) = z, \theta = \tau \right\} = \frac{\int_{\{u < z_{\tau_j^c}, v < a\}} \lambda_{(s, x_{\tau_j^c}) | x_{\tau_j}, z_{\tau_j}}(v, u) dudv}{\int_{\{u < z_{\tau_j^c}\}} \lambda_{x_{\tau_j^c} | x_{\tau_j}, z_{\tau_j}}(u) du}.$$

259

It is clear from (3) that the conditional random field $Z \mid \{Z(x) = z\}$ is not max-stable.

260

2.2. Distribution of the extremal functions

261

In this section we derive closed forms for the intensity function $\lambda_x(z)$ and the conditional
 262 intensity function $\lambda_{s|x, z}(u)$ for two widely used max-stable processes; the Brown–Resnick
 263 (Brown & Resnick, 1977; Kabluchko et al., 2009) and the Schlather (Schlather, 2002) processes.

264

Details of the derivations of these closed forms are given in the Appendix.

265

266

267

289 The Brown–Resnick process corresponds to the case where $Y(x) = \exp\{W(x) - \gamma(x)\}$, $x \in$
 290 \mathbb{R}^d , in (1) with W a centered Gaussian process with stationary increments, semi variogram γ
 291 and such that $W(o) = 0$ almost surely. For $x \in \mathcal{X}^k$ and provided the covariance matrix Σ_x of
 292 the random vector $W(x)$ is positive definite, the intensity function is

$$293 \lambda_x(z) = C_x \exp\left(-\frac{1}{2} \log z^T Q_x \log z + L_x \log z\right) \prod_{i=1}^k z_i^{-1}, \quad z \in (0, \infty)^k,$$

294 with $\mathbf{1}_k = (1)_{i=1, \dots, k}$, $\sigma_x^2 = \{\sigma^2(x_i)\}_{i=1, \dots, k}$,

$$295 Q_x = \Sigma_x^{-1} - \frac{\Sigma_x^{-1} \mathbf{1}_k \mathbf{1}_k^T \Sigma_x^{-1}}{\mathbf{1}_k^T \Sigma_x^{-1} \mathbf{1}_k}, \quad L_x = \frac{1}{2} \left(\frac{\mathbf{1}_k^T \Sigma_x^{-1} \sigma_x^2 - 2 \mathbf{1}_k^T}{\mathbf{1}_k^T \Sigma_x^{-1} \mathbf{1}_k} - \sigma_x^{2T} \right) \Sigma_x^{-1},$$

$$296 C_x = (2\pi)^{(1-k)/2} |\Sigma_x|^{-1/2} (\mathbf{1}_k^T \Sigma_x^{-1} \mathbf{1}_k)^{-1/2} \exp \left\{ \frac{1}{2} \frac{(\mathbf{1}_k^T \Sigma_x^{-1} \sigma_x^2 - 1)^2}{\mathbf{1}_k^T \Sigma_x^{-1} \mathbf{1}_k} - \frac{1}{2} \sigma_x^{2T} \Sigma_x^{-1} \sigma_x^2 \right\},$$

297 and for all $(s, x) \in \mathcal{X}^{m+k}$, $(u, z) \in (0, \infty)^{m+k}$ and provided the covariance matrix $\Sigma_{(s,x)}$ is pos-
 298 itive definite, the conditional intensity function corresponds to a multivariate log-normal proba-
 299 bility density function

$$300 \lambda_{s|x,z}(u) = (2\pi)^{-m/2} |\Sigma_{s|x}|^{-1/2} \exp \left\{ -\frac{1}{2} (\log u - \mu_{s|x,z})^T \Sigma_{s|x}^{-1} (\log u - \mu_{s|x,z}) \right\} \prod_{i=1}^m u_i^{-1},$$

301 where $\mu_{s|x,z} \in \mathbb{R}^m$ and $\Sigma_{s|x}$ are the mean and covariance matrix of the underlying normal dis-
 302 tribution and are given by

$$303 \Sigma_{s|x}^{-1} = J_{m,k}^T Q_{(s,x)} J_{m,k}, \quad \mu_{s|x,z} = \left\{ L_{(s,x)} J_{m,k} - \log z^T \tilde{J}_{m,k}^T Q_{(s,x)} J_{m,k} \right\} \Sigma_{s|x},$$

304 with

$$305 J_{m,k} = \begin{bmatrix} \text{Id}_m \\ 0_{k,m} \end{bmatrix}, \quad \tilde{J}_{m,k} = \begin{bmatrix} 0_{m,k} \\ \text{Id}_k \end{bmatrix},$$

306 where Id_k denotes the $k \times k$ identity matrix and $0_{m,k}$ the $m \times n$ null matrix.

307 The Schlather process considers the case where $Y(x) = (2\pi)^{1/2} \max\{0, \varepsilon(x)\}$, $x \in \mathbb{R}^d$, in (1)
 308 with ε a standard Gaussian process with correlation function ρ . The associated point process Φ
 309 is not regular and it is more convenient to consider the equivalent representation where $Y(x) =$
 310

311
 312
 313
 314
 315

337 $(2\pi)^{1/2}\varepsilon(x)$, $x \in \mathbb{R}^d$. For $x \in \mathcal{X}^k$ and provided the covariance matrix Σ_x of the random vector
 338 $\varepsilon(x)$ is positive definite, the intensity function is

$$339 \lambda_x(z) = \pi^{-(k-1)/2} |\Sigma_x|^{-1/2} a_x(z)^{-(k+1)/2} \Gamma\left(\frac{k+1}{2}\right), \quad z \in \mathbb{R}^k,$$

340 where $a_x(z) = z^T \Sigma_x^{-1} z$.

341 For $(s, x) \in \mathcal{X}^{m+k}$, $(u, z) \in \mathbb{R}^{m+k}$ and provided that the covariance matrix $\Sigma_{(s,x)}$ is positive
 342 definite, the conditional intensity function $\lambda_{s|x,z}(u)$ corresponds to the density of a multivariate
 343 Student distribution with $k+1$ degrees of freedom, location parameter $\mu = \Sigma_{s:x} \Sigma_x^{-1} z$, and scale
 344 matrix

$$345 \tilde{\Sigma} = \frac{a_x(z)}{k+1} (\Sigma_s - \Sigma_{s:x} \Sigma_x^{-1} \Sigma_{x:s}), \quad \Sigma_{(s,x)} = \begin{bmatrix} \Sigma_s & \Sigma_{s:x} \\ \Sigma_{x:s} & \Sigma_x \end{bmatrix}.$$

349 3. MARKOV CHAIN MONTE CARLO SAMPLER

350 The previous section introduced a procedure to get realizations from the regular conditional
 351 distribution of max-stable processes. This sampling scheme amounts to sample from a discrete
 352 distribution whose state space corresponds to all possible partitions of the set of conditioning
 353 points, see Theorem 1 step 1. Hence, even for a moderate number k of conditioning locations,
 354 the state space \mathcal{P}_k becomes very large and the distribution $\pi_x(z, \cdot)$ cannot be computed. It turns
 355 out that a Gibbs sampler is especially convenient.

356 For $\tau \in \mathcal{P}_k$, let τ_{-j} be the restriction of τ to the set $\{x_1, \dots, x_k\} \setminus \{x_j\}$. Our goal is to
 357 simulate from the conditional distribution

$$358 \text{pr}(\theta \in \cdot \mid \theta_{-j} = \tau_{-j}), \quad (4)$$

359 where $\theta \in \mathcal{P}_k$ is a random partition which follows the target distribution $\pi_x(z, \cdot)$.

360

361

362

363

385 Since the number of possible updates is always less than k , a combinatorial explosion is
 386 avoided. Indeed for $\tau \in \mathcal{P}_k$ of size ℓ , the number of partitions $\tau^* \in \mathcal{P}_k$ such that $\tau_{-j}^* = \tau_{-j}$
 387 for some $j \in \{1, \dots, k\}$ is

$$b^+ = \begin{cases} \ell & \text{if } \{x_j\} \text{ is a partitioning set of } \tau, \\ \ell + 1 & \text{if } \{x_j\} \text{ is not a partitioning set of } \tau, \end{cases}$$

388 since the point x_j may be reallocated to any partitioning set of τ_{-j} or to a new one.
 389

390 To illustrate consider the set $\{x_1, x_2, x_3\}$ and let $\tau = (\{x_1, x_2\}, \{x_3\})$. Then the possible
 391 partitions τ^* such that $\tau_{-2}^* = \tau_{-2}$ are $(\{x_1, x_2\}, \{x_3\})$, $(\{x_1\}, \{x_2\}, \{x_3\})$, $(\{x_1\}, \{x_2, x_3\})$,
 392 while there exists only two partitions such that $\tau_{-3}^* = \tau_{-3}$, i.e., $(\{x_1, x_2\}, \{x_3\})$, $(\{x_1, x_2, x_3\})$.
 393

394 The distribution (4) has nice properties. Since for all $\tau^* \in \mathcal{P}_k$ such that $\tau_{-j}^* = \tau_{-j}$ we have
 395

$$\text{pr}[\theta = \tau^* \mid \theta_{-j} = \tau_{-j}] = \frac{\pi_x(z, \tau^*)}{\sum_{\tilde{\tau} \in \mathcal{P}_k} \pi_x(z, \tilde{\tau}) \mathbf{1}_{\{\tilde{\tau}_{-j} = \tau_{-j}\}}} \propto \frac{\prod_{j=1}^{|\tau^*|} w_{\tau^*, j}}{\prod_{j=1}^{|\tau|} w_{\tau, j}}, \quad (5)$$

396 where
 397

$$w_{\tau, j} = \lambda_{x_{\tau_j}}(z_{\tau_j}) \int_{\{u < z_{\tau_j^c}\}} \lambda_{x_{\tau_j^c} | x_{\tau_j}, z_{\tau_j}}(u) du.$$

398 Since many factors cancel out on the right hand side of (5), the Gibbs sampler is especially
 399 convenient.
 400

401 The most computationally demanding part of (5) is the evaluation of the integral
 402

$$\int_{\{u < z_{\tau_j^c}\}} \lambda_{x_{\tau_j^c} | x_{\tau_j}, z_{\tau_j}}(u) du.$$

403 For the Brown–Resnick and Schlather processes, we follow the lines of Genz (1992) and compute
 404 these probabilities using a separation of variables method which provides a transformation of the
 405 original integration problem to the unit hyper-cube. Further a quasi Monte Carlo scheme and
 406 antithetic variable sampling is used to improve efficiency.
 407
 408
 409

410
 411

433 Since it is not obvious how to implement a Gibbs sampler whose target distribution has support
 434 \mathcal{P}_k , the remainder of this section gives practical details. For any fixed locations $x_1, \dots, x_k \in$
 435 \mathcal{X} , we first describe how each partition of $\{x_1, \dots, x_k\}$ is stored. To illustrate consider the set
 436 $\{x_1, x_2, x_3\}$ and the partition $(\{x_1, x_2\}; \{x_3\})$. This partition is defined as $(1, 1, 2)$, indicating
 437 that x_1 and x_2 belong to the same partitioning set labeled 1 and x_3 belongs to the partitioning set
 438 2. There exist several equivalent notations for this partition: for example one can use $(2, 2, 1)$ or
 439 $(1, 1, 3)$. Since there is a one-one mapping between \mathcal{P}_k and the set

$$440 \quad \mathcal{P}_k^* = \left\{ (a_1, \dots, a_k) : i \in \{2, \dots, k\}, 1 = a_1 \leq a_i \leq \max_{1 \leq j < i} a_j + 1, a_i \in \mathbb{Z} \right\},$$

442 we shall restrict our attention to the partitions that live in \mathcal{P}_k^* and going back to our example we
 443 see that $(1, 1, 2)$ is valid but $(2, 2, 1)$ and $(1, 1, 3)$ are not.

444 For $\tau \in \mathcal{P}_k^*$ of size ℓ , let $r_1 = \sum_{i=1}^k 1_{\{\tau_i = a_j\}}$ and $r_2 = \sum_{i=1}^k 1_{\{\tau_i = b\}}$, i.e., the number of
 445 conditioning locations that belong to the partitioning sets a_j and b where $b \in \{1, \dots, b^+\}$ with

$$446 \quad b^+ = \begin{cases} \ell & (r_1 = 1), \\ \ell + 1 & (r_1 \neq 1). \end{cases}$$

449 Then the conditional probability distribution (5) satisfies

$$450 \quad \text{pr}(\tau_j = b \mid \tau_i = a_i, i \neq j) \propto \begin{cases} 1 & (b = a_j), & (6a) \\ w_{\tau^*, b} / (w_{\tau, b} w_{\tau, a_j}) & (r_1 = 1, r_2 \neq 0, b \neq a_j), & (6b) \\ w_{\tau^*, b} w_{\tau^*, a_j} / (w_{\tau, b} w_{\tau, a_j}) & (r_1 \neq 1, r_2 \neq 0, b \neq a_j), & (6c) \\ w_{\tau^*, b} w_{\tau^*, a_j} / w_{\tau, a_j} & (r_1 \neq 1, r_2 = 0, b \neq a_j), & (6d) \end{cases}$$

454 where $\tau^* = (a_1, \dots, a_{j-1}, b, a_{j+1}, \dots, a_k)$. Although τ^* may not belong to \mathcal{P}_k^* , it corresponds
 455 to a unique partition of \mathcal{P}_k and we can use the bijection $\mathcal{P}_k \rightarrow \mathcal{P}_k^*$ to recode τ^* into an element
 456 of \mathcal{P}_k^* . In (6a)–(6d) the event $\{r_1 = 1, r_2 = 0, b \neq a_j\}$ is missing since $\{r_1 = 1, r_2 = 0\}$ implies
 457

Table 1. *Sample path properties of the max-stable models. For the Brown–Resnick model, the variogram parameters are set to ensure that the extremal coefficient function satisfies $\theta(115) = 1.7$ while the correlation function parameters are set to ensure that $\theta(100) = 1.5$ for the Schlather model.*

	Brown–Resnick: $\gamma(h) = (h/\lambda)^\kappa$			Schlather: $\rho(h) = \exp\{-(h/\lambda)^\kappa\}$		
	γ_1 : Very wiggly	γ_2 : Wiggly	γ_3 : Smooth	ρ_1 : Very wiggly	ρ_2 : Wiggly	ρ_3 : Smooth
λ	25	54	69	208	144	128
κ	0.5	1.0	1.5	0.5	1.0	1.5

that $\tau^* = \tau$, where the equality has to be understood in terms of elements of \mathcal{P}_k , and this case has been already taken into account with (6a).

Once these conditional weights have been computed, the Gibbs sampler proceeds by updating each element of τ successively. We use a random scan implementation of the Gibbs sampler (Liu et al., 1995). More precisely, one iteration of the random scan Gibbs sampler selects an element of τ at random according to a given distribution, say $p = (p_1, \dots, p_k)$, and then updates this element. Throughout this paper we will use the uniform random scan Gibbs sampler for which the selection distribution is assumed to be a discrete uniform distribution, i.e., $p = (k^{-1}, \dots, k^{-1})$.

4. SIMULATION STUDY

In this section we check if our algorithm is able to produce realistic conditional simulations of Brown–Resnick and Schlather processes. For each model, we consider three different sample path properties, as summarized in Table 1. These configurations were chosen such that the spatial dependence structures are similar to our applications in Section 5.

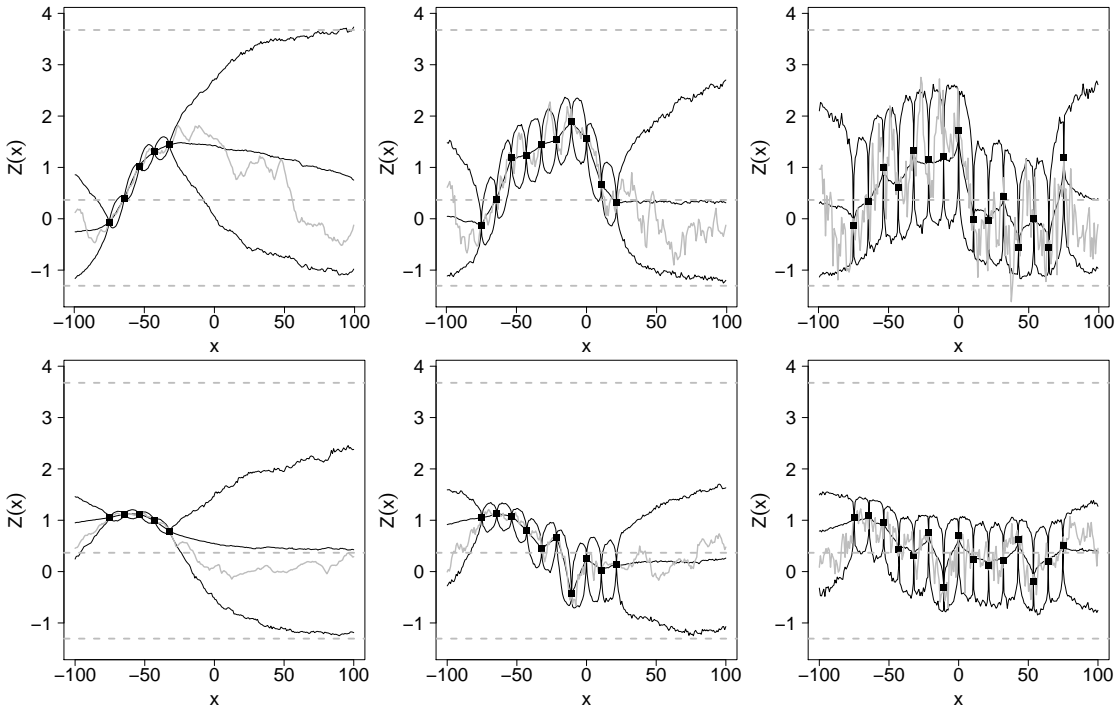


Fig. 1. Pointwise sample quantiles estimated from 1000 conditional simulations of max-stable processes with standard Gumbel margins with $k = 5, 10, 15$ conditioning locations. The top row shows results for the Brown-Resnick models with semi variograms $\gamma_3, \gamma_2, \gamma_1$, from left to right. The bottom row shows results for the Schlather models with correlation functions ρ_3, ρ_2, ρ_1 , from left to right. The solid black lines shows the pointwise 0.025, 0.5, 0.975 sample quantiles and the dashed grey lines that of a standard Gumbel distribution. The squares show the conditional points $\{(x_i, z_i)\}_{i=1, \dots, k}$. The solid grey lines correspond the simulated paths used to get the conditioning events.

In order to check if our sampling procedure is accurate and given a single conditional event $\{Z(x) = z\}$ for each configuration, we generated 1000 conditional realizations with standard Gumbel margins. Figure 1 shows the pointwise sample quantiles obtained from these 1000 sim-

Table 2. Computational timings for conditional simulations of max-stable processes on a 50×50 grid defined on the square $[0, 100 \times 2^{1/2}]^2$ for a varying number k of conditioning locations uniformly distributed over the region. The timings, in seconds, are mean values over 100 conditional simulations; standard deviations are reported in brackets.

	Brown–Resnick: $\gamma(h) = (h/25)^{0.5}$				Schlather: $\rho(h) = \exp\{-(h/208)^{0.50}\}$			
	Step 1	Step 2	Step 3	Overall	Step 1	Step 2	Step 3	Overall
$k = 5$	0.21 (0.01)	49 (11)	1.4 (0.1)	50 (11)	1.40 (0.02)	1.9 (0.7)	0.9 (0.3)	4.2 (0.8)
$k = 10$	8 (2)	76 (18)	1.4 (0.1)	85 (19)	12 (4)	2.4 (0.8)	1.0 (0.3)	15 (4)
$k = 25$	95 (38)	117 (30)	1.4 (0.1)	214 (61)	86 (42)	4 (1)	1.0 (0.3)	90 (43)
$k = 50$	583 (313)	348 (391)	1.5 (0.1)	931 (535)	367 (222)	62 (113)	1.0 (0.3)	430 (262)

Conditional simulations with $k = 5$ do not use a Gibbs sampler.

ulated paths and compares them to unit Gumbel quantiles. As expected the conditional sample paths inherit the regularity driven by the shape parameter κ and there is less variability in regions close to conditioning locations. Since the considered Brown–Resnick processes are ergodic (Kablichko and Schlather, 2010), for regions far away from any conditioning location the sample quantiles converges to that of a standard Gumbel distribution indicating that the conditional event has no influence. This is not the case for the non-ergodic Schlather processes. Most of the time the sample paths used to get the conditional events belong to the 95% pointwise confidence intervals, corroborating that our sampling procedure seems to be accurate.

Table 2 gives computational timings for conditional simulations of max-stable processes on a 50×50 grid with a varying number of conditioning locations. Due to the combinatorial complexity of the partition set \mathcal{P}_k , the timings increase rapidly with respect to the number of conditioning points k . It is however reassuring that the algorithm is tractable when $k \in \{1, \dots, 50\}$; hence covering many practical situations and applications.

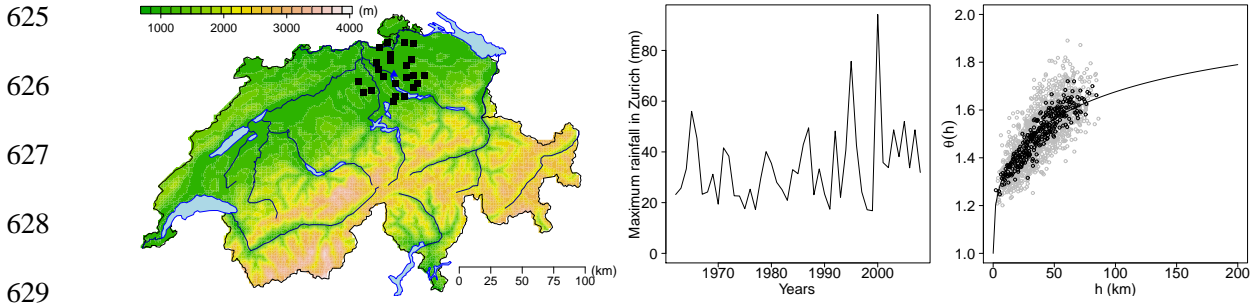


Fig. 2. Left: Map of Switzerland showing the stations of the 24 rainfall gauges used for the analysis, with an insert showing the altitude. The station marked with a triangle corresponds to Zurich. Middle: Summer maximum rainfall values for 1962–2008 at Zurich. Right: Comparison between the pairwise extremal coefficient estimates for the 51 original weather stations and the extremal coefficient function derived from a fitted Brown–Resnick processes having semi variogram $\gamma(h) = (h/\lambda)^\kappa$. The grey points are pairwise estimates; the black ones are binned estimates and the curve is the fitted extremal coefficient function.

5. APPLICATION

5.1. *Extreme precipitations around Zurich*

In this section we obtain conditional simulations of extreme precipitation fields. The data considered here were previously analyzed by Davison et al. (2011) who showed that Brown–Resnick processes were one of the most competitive models among various statistical models for spatial extremes.

The data are summer maximum rainfall for the years 1962–2008 at 51 weather stations in the Plateau region of Switzerland, provided by the national meteorological service, MeteoSuisse. To ensure strong dependence between the conditioning locations, we consider as conditional locations the 24 weather stations that are at most 30km apart from Zurich and set as the conditional

Table 3. *Distribution of the partition size for the rainfall data estimated from a simulated Markov chain of length 15000*

Partition size	1	2	3	4	5	6	7–24
Empirical probabilities (%)	66.2	28.0	4.8	0.5	0.2	0.2	<0.05

values the rainfall amounts recorded in the year 2000, the year of the largest precipitation event ever recorded in Zurich between 1962–2008, see Figure 2. The largest and smallest distances between the conditioning locations are around 55km and just over 4km respectively.

A Brown–Resnick process having semi variogram $\gamma(h) = (h/\lambda)^\kappa$ has to be fitted and the maximum pairwise likelihood estimator introduced by Padoan et al. (2010) was used to simultaneously fit the marginal parameters and the spatial dependence parameters λ and κ . In accordance with Davison et al. (2011), the marginal parameters were described by $\eta(x) = \beta_{0,\eta} + \beta_{1,\eta}\text{lon}(x) + \beta_{2,\eta}\text{lat}(x)$, $\sigma(x) = \beta_{0,\sigma} + \beta_{1,\sigma}\text{lon}(x) + \beta_{2,\sigma}\text{lat}(x)$, $\xi(x) = \beta_{0,\xi}$, where $\eta(x), \sigma(x), \xi(x)$ are the location, scale and shape parameters of the generalized extreme value distribution and $\text{lon}(x), \text{lat}(x)$ the longitude and latitude of the stations at which the data are observed. The maximum pairwise likelihood estimates for λ and κ are 38 (14) and 0.69 (0.07) and give a practical extremal range, i.e., the distance h_+ such that $\theta(h_+) = 1.7$, of around 115km, see the right panel of Figure 2.

Table 3 shows the distribution of the partition size estimated from a Markov chain of length 15000. Around 65% of the time the summer maxima observed at the 24 conditioning locations were a consequence of a single extremal function, i.e., only one storm event, and around 30% of the time a consequence of two different storms. Since the simulated Markov chain keeps a trace of all the simulated partitions, we looked at the partitions of size two and saw that around 65% of the time, at least one of the four up–north conditioning locations was impacted by one extremal function while the remaining 20 locations were always influenced by another one.

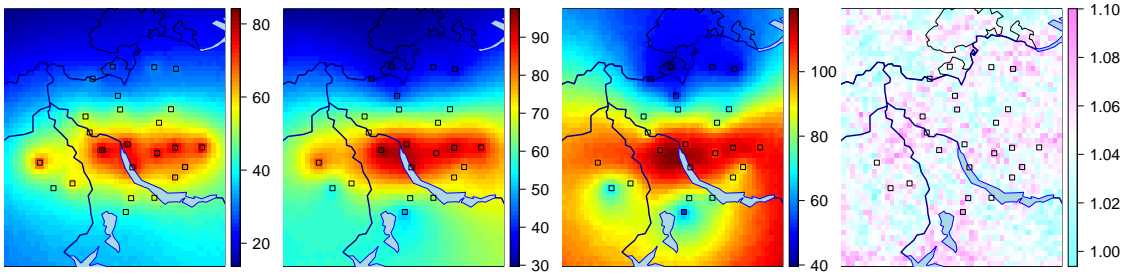


Fig. 3. From left to right, maps on a 50×50 grid of the pointwise 0.025, 0.5 and 0.975 sample quantiles for rainfall (mm) obtained from 10000 conditional simulations of Brown–Resnick processes having semi variogram $\gamma(h) = (h/38)^{0.69}$. The right most panel plots the ratio of the pointwise confidence intervals with and without taking into account the parameter estimate uncertainties. The squares show the conditional locations.

Figure 3 plots the pointwise 0.025, 0.5 and 0.975 sample quantiles obtained from 10000 conditional simulations of our fitted Brown–Resnick process. The conditional median provides a point estimate for the rainfall at an ungauged location and the 0.025 and 0.975 conditional quantiles a 95% pointwise confidence interval. As indicated by our simulation study, see Figure 1, the shape parameter κ has a major impact on the regularity of paths and on the width of the confidence interval. The value $\hat{\kappa} \approx 0.69$ corresponds to very wiggly sample paths and wider confidence intervals. To assess the impact of parameter uncertainties on conditional simulations, the ratio of the width of the confidence intervals with or without parameter uncertainty is shown in the right panel of Figure 3. The uncertainties were taken into account by sampling from the asymptotic distribution of the maximum composite likelihood estimator and draw one conditional simulation for each realization. These ratios show no clear spatial pattern and the width of the confidence interval is increased by an amount of at most 10%.

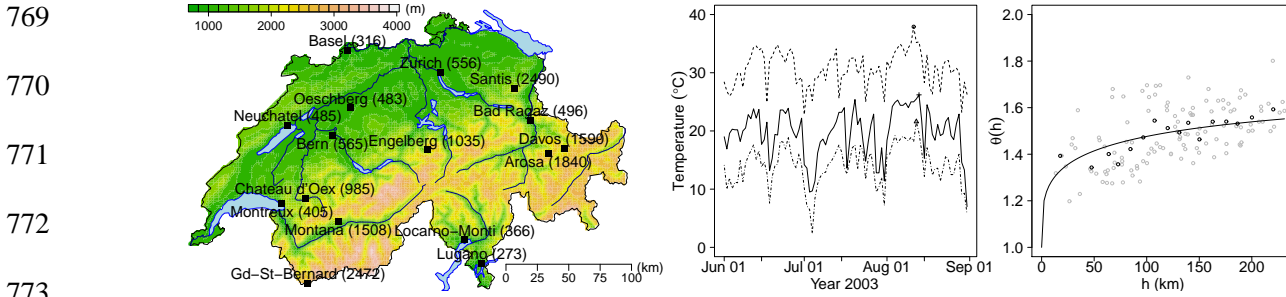


Fig. 4. Left: Topographical map of Switzerland showing the sites and altitudes in metres above sea level of 16 weather stations for which annual maxima temperature data are available. Middle: Times series of the daily maxima temperatures at the 16 weather stations for year 2003. The 'o', '+' and 'x' symbols indicate the annual maxima that occurred the 11th, 12th and 13th of August respectively. Right: Comparison between the fitted extremal coefficient function from a Schlather process (solid red line) and the pairwise extremal coefficient estimates (gray circles). The black circles denote binned estimates with 16 bins.

5.2. Extreme temperatures in Switzerland

In this section we apply our results to get conditional simulations of extreme temperature fields. The data considered here were previously analyzed by Davison and Gholam-Rezaee (2011) and consist in annual maximum temperatures recorded at 16 sites in Switzerland during the period 1961–2005, see Figure 4.

Following the work of Davison and Gholam-Rezaee (2011), we fit a Schlather process with an isotropic powered exponential correlation function and trend surfaces $\eta(x) = \beta_{0,\eta} + \beta_{1,\eta}\text{alt}(x)$, $\sigma(x) = \beta_{0,\sigma}$, $\xi(x) = \beta_{0,\xi} + \beta_{1,\xi}\text{alt}(x)$, where $\text{alt}(x)$ denotes the altitude above mean sea level in kilometres and $\{\eta(x), \sigma(x), \xi(x)\}$ are the location, scale and shape parameters of the generalized extreme value distribution at location x . The spatial dependence parameter estimates are

Table 4. *Distribution of the partition size for the temperature**data estimated from a Markov chain of length 10000*

Partition size	1	2	3	4	5–16
Empirical probabilities (%)	2.47	21.55	64.63	10.74	0.61

$\hat{\lambda} = 260$ (149) and $\hat{\kappa} = 0.52$ (0.12) and the corresponding fitted extremal coefficient function, similar to some extent to our test case ρ_3 in Section 4, is shown in the right panel of Figure 4.

In year 2003, western Europe was hit by a severe heat wave believed to be the hottest one ever recorded since at most 1540 (“2003 European heat wave”, Wikipedia: The Free Encyclopedia). Switzerland was largely impacted by this severe extreme event since the nation wide record temperature of 41.5°C was recorded that year in Grono, Graubunden, near Lugano. Consequently for our analysis we use as conditional event the maxima temperatures observed in summer 2003, see Figure 4. Based on the fitted Schlather model, we simulate a Markov chain of effective length 10000 with a burn-in period of length 500 and a thinning lag of 100 iterations. The distribution of the partition size estimated from these Markov chains is shown in Table 4. We can see that around 90% of the time the conditional realizations were a consequence of at most three extremal functions. Since our original observations were not summer maxima but maximum daily values, a close inspection of the times series in year 2003 reveals that the hottest temperatures occurred between the 11th and 13th of August, see Figure 4, and, to some extent, corroborates the distribution of Table 4.

Figure 5 shows the 0.025, 0.5 and 0.975 pointwise sample quantiles obtained from 10000 conditional simulations on a 64×64 grid. As expected, we can see that the largest temperatures occurred in the plateau region of Switzerland while temperatures were appreciably cooler in the Alps. The right panel of Figure 5 shows the difference between the pointwise conditional medians and the pointwise unconditional medians estimated from the fitted trend surfaces. The

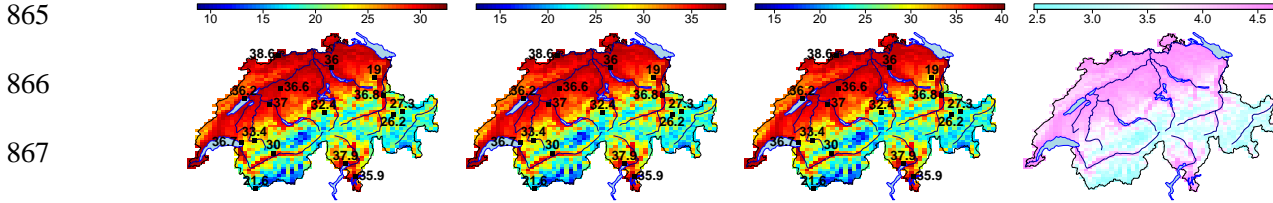


Fig. 5. From left to right: Maps on a 64×64 grid of the pointwise 0.025, 0.5 and 0.975 sample quantiles for temperature ($^{\circ}\text{C}$) obtained from 10000 conditional simulations of the fitted Schlather process. The squares show the conditional locations and the associated conditional values. The right most panel shows temperature anomalies, i.e., the difference between the pointwise conditional and unconditional medians.

differences range between 2.5°C and 4.75°C and the largest deviations occur in the plateau region of Switzerland.

ACKNOWLEDGEMENTS

M. Ribatet was partly funded by the MIRACCLE-GICC and McSim ANR projects. The authors thank MeteoSuisse and Dr. S. A. Padoan for providing the precipitation data and Prof. A. C. Davison and Dr. M. M. Gholam-Rezaee for providing the temperature data set.

APPENDIX

The Brown–Resnick model

For all $x \in \mathcal{X}^k$ and Borel set $A \subset \mathbb{R}^k$

$$\Lambda_x(A) = \int_0^{\infty} \text{pr} [\zeta \exp\{W(x) - \gamma(x)\} \in A] \zeta^{-2} d\zeta = \int_0^{\infty} \int_{\mathbb{R}^k} 1_{\{\zeta \exp\{y - \gamma(x)\} \in A\}} f_x(y) dy \zeta^{-2} d\zeta,$$

where f_x denotes the density of the random vector $W(x)$, i.e., a centered Gaussian random vector with covariance matrix Σ_x and variance $2\gamma(x)$. The change of variables $z = \zeta \exp\{y - \gamma(x)\}$ and $r = \log \zeta$

913 yields

$$914 \quad \Lambda_x(A) = \int_{-\infty}^{\infty} \int_A f_x \{ \log z - r + \gamma(x) \} \prod_{i=1}^k z_i^{-1} dz e^{-r} dr = \int_A \lambda_x(z) dz$$

915

with

916

$$917 \quad \lambda_x(z) = \prod_{i=1}^k z_i^{-1} \int_{-\infty}^{\infty} f_x \{ \log z - r + \gamma(x) \} e^{-r} dr.$$

918

Since

919

$$920 \quad f_x \{ \log z - r + \gamma(x) \} e^{-r} = (2\pi)^{-k/2} |\Sigma_x|^{-1/2} \exp \left\{ -\frac{1}{2} P(r) \right\},$$

921

with

922

$$P(r) = r^2 1_k^T \Sigma_x^{-1} 1_k - 2r [1_k^T \Sigma_x^{-1} \{ \log z + \gamma(x) \} - 1] + \{ \log z + \gamma(x) \}^T \Sigma_x^{-1} \{ \log z + \gamma(x) \},$$

923

standard computations for Gaussian integrals give

924

$$925 \quad \lambda_x(z) = C_x \exp \left(-\frac{1}{2} \log z^T Q_x \log z + L_x \log z \right) \prod_{i=1}^k z_i^{-1}.$$

926

The conditional intensity function is

927

$$928 \quad \lambda_{s|x,z}(u) = \frac{C_{(s,x)}}{C_x} \exp \left\{ -\frac{1}{2} \log(u, z)^T Q_{(s,x)} \log(u, z) + L_{(s,x)} \log(u, z) + \frac{1}{2} \log z^T Q_x \log z - L_x \log z \right\} \prod_{i=1}^m u_i^{-1},$$

929

and since $\log(u, z) = J_{m,k} \log u + \tilde{J}_{m,k} \log z$, it is not difficult to show that

930

$$931 \quad \lambda_{s|x,z}(u) = \frac{C_{(s,x)}}{C_x} \exp \left\{ -\frac{1}{2} (\log u - \mu_{s|x,z})^T \Sigma_{s|x}^{-1} (\log u - \mu_{s|x,z}) \right\} \prod_{i=1}^m u_i^{-1}.$$

932

Finally, the relation $C_{(s,x)}/C_x = (2\pi)^{-m/2} |\Sigma_{s|x}|^{-1/2}$ is a simple consequence of the normalization

933

$$\int \lambda_{s|x,z}(u) du = 1.$$

934

The Schlather model

935

For all $x \in \mathcal{X}^k$ and Borel set $A \subset \mathbb{R}^k$

936

$$937 \quad \Lambda_x(A) = \int_0^{\infty} \text{pr}[\sqrt{2\pi}\zeta\varepsilon(x) \in A] \zeta^{-2} d\zeta = \int_0^{\infty} \int_{\mathbb{R}^k} 1_{\{\sqrt{2\pi}\zeta y \in A\}} f_{\mathbf{x}}(y) dy \zeta^{-2} d\zeta,$$

938

939

961 where f_x denotes the density of the random vector $\varepsilon(x)$, i.e., a centered Gaussian random vector with
 962 covariance matrix Σ_x . The change of variable $z = \sqrt{2\pi}\zeta y$ gives

$$\begin{aligned}
 963 \quad \Lambda_x(A) &= (2\pi)^{-k/2} \int_0^\infty \int_A f_x \left(\frac{z}{\sqrt{2\pi}\zeta} \right) \zeta^{-(k+2)} dz d\zeta \\
 964 &= (2\pi)^{-k} |\Sigma_x|^{-1/2} \int_0^\infty \int_A \exp \left(-\frac{1}{4\pi\zeta^2} z^T \Sigma_x^{-1} z \right) \zeta^{-(k+2)} dz d\zeta \\
 965 &= (2\pi)^{-k} |\Sigma_x|^{-1/2} \int_A \frac{2\pi}{z^T \Sigma_x^{-1} z} \mathbb{E}[X^{k-1}] dz, \quad X \sim \text{Weibull} \left(\sqrt{\frac{4\pi}{z^T \Sigma_x^{-1} z}}, 2 \right) \\
 966 &= (2\pi)^{-k} |\Sigma_x|^{-1/2} \int_A \frac{2\pi}{z^T \Sigma_x^{-1} z} \left(\frac{4\pi}{z^T \Sigma_x^{-1} z} \right)^{(k-1)/2} \Gamma \left(\frac{k+1}{2} \right) dz \\
 967 &= \int_A \lambda_x(z) dz,
 \end{aligned}$$

969 where $\lambda_x(z) = \pi^{-(k-1)/2} |\Sigma_x|^{-1/2} a_x(z)^{-(k+1)/2} \Gamma \{(k+1)/2\}$ and $a_x(z) = z^T \Sigma_x^{-1} z$.

970 For all $u \in \mathbb{R}^m$ the conditional intensity function is

$$971 \quad \lambda_{s|x,z}(u) = \pi^{-m/2} \frac{|\Sigma_{(s,x)}|^{-1/2}}{|\Sigma_x|^{-1/2}} \left\{ \frac{a_{(s,x)}(u,z)}{a_x(z)} \right\}^{-(m+k+1)/2} a_x(z)^{-m/2} \frac{\Gamma \left(\frac{m+k+1}{2} \right)}{\Gamma \left(\frac{k+1}{2} \right)}.$$

972 We start by focusing on the ratio $a_{(s,x)}(u,z)/a_x(z)$. Since

$$973 \quad \begin{bmatrix} \Sigma_s & \Sigma_{s:x} \\ \Sigma_{x:s} & \Sigma_x \end{bmatrix}^{-1} = \begin{bmatrix} (\Sigma_s - \Sigma_{s:x} \Sigma_x^{-1} \Sigma_{x:s})^{-1} & -(\Sigma_s - \Sigma_{s:x} \Sigma_x^{-1} \Sigma_{x:s})^{-1} \Sigma_{s:x} \Sigma_x^{-1} \\ -\Sigma_x^{-1} \Sigma_{x:s} (\Sigma_s - \Sigma_{s:x} \Sigma_x^{-1} \Sigma_{x:s})^{-1} \Sigma_x^{-1} + \Sigma_x^{-1} \Sigma_{x:s} (\Sigma_s - \Sigma_{s:x} \Sigma_x^{-1} \Sigma_{x:s})^{-1} \Sigma_{s:x} \Sigma_x^{-1} & \end{bmatrix},$$

975 straightforward algebra shows that

$$976 \quad \frac{a_{(s,x)}(u,z)}{a_x(z)} = 1 + \frac{(u - \mu)^T \tilde{\Sigma}^{-1} (u - \mu)}{k+1}, \quad \mu = \Sigma_{s:x} \Sigma_x^{-1} z, \quad \tilde{\Sigma} = \frac{a_x(z)}{k+1} (\Sigma_s - \Sigma_{s:x} \Sigma_x^{-1} \Sigma_{x:s}).$$

978 We now try to simplify the ratio $|\Sigma_{(s,x)}|/|\Sigma_x|$. Using the fact that

$$979 \quad \Sigma_{(s,x)} = \begin{bmatrix} \Sigma_s & \Sigma_{s:x} \\ \Sigma_{x:s} & \Sigma_x \end{bmatrix} = \begin{bmatrix} \text{Id}_m & \Sigma_{s:x} \\ 0_{k,m} & \Sigma_x \end{bmatrix} \begin{bmatrix} \Sigma_s - \Sigma_{s:x} \Sigma_x^{-1} \Sigma_{x:s} & 0_{m,k} \\ \Sigma_x^{-1} \Sigma_{x:s} & \text{Id}_k \end{bmatrix},$$

980 combined with some more algebra yields

$$981 \quad \frac{|\Sigma_{(s,x)}|}{|\Sigma_x|} = |\Sigma_s - \Sigma_{s:x} \Sigma_x^{-1} \Sigma_{x:s}| = \left\{ \frac{k+1}{a_x(z)} \right\}^m |\tilde{\Sigma}|.$$

983 Using the two previous results it is easily found that

$$984 \quad \lambda_{s|x,z}(u) = \pi^{-m/2} (k+1)^{-m/2} |\tilde{\Sigma}|^{-1/2} \left\{ 1 + \frac{(u - \mu)^T \tilde{\Sigma}^{-1} (u - \mu)}{k+1} \right\}^{-(m+k+1)/2} \frac{\Gamma \left(\frac{m+k+1}{2} \right)}{\Gamma \left(\frac{k+1}{2} \right)},$$

985

986

987

1009 which corresponds to the density of a multivariate Student distribution with the expected parameters.

1010

1011

REFERENCES

1012

BROWN, B. M. & RESNICK, S. I. (1977). Extreme values of independent stochastic processes. *J. Appl. Prob.* **14**,
1013 732–739.

1014

BUIHAND, T. A., DE HAAN, L. & ZHOU, C. (2008). On spatial extremes: With application to a rainfall problem.
1015 *Annals of Applied Statistics* **2**, 624–642.

1016

CHILÈS, J.-P. & DELFINER, P. (1999). *Geostatistics: Modelling Spatial Uncertainty*. New York: Wiley.

1017

COOLEY, D., NAVEAU, P. & PONCET, P. (2006). Variograms for spatial max-stable random fields. In *Dependence*
1018 *in Probability and Statistics*, vol. 187 of *Lecture Notes in Statistics*. New York: Springer, pp. 373–390.

1019

DAVIS, R. & RESNICK, S. (1989). Basic properties and prediction of max-arma processes. *Advances in Applied*
1020 *Probability* **21**, 781–803.

1021

DAVIS, R. & RESNICK, S. (1993). Prediction of stationary max-stable processes. *Annals Of Applied Probability* **3**,
1022 497–525.

1023

DAVISON, A. C. & GHOLAM-REZAEI, M. M. (2011). Geostatistics of extremes. *Proceedings of the Royal Society*
1024 *A: Mathematical, Physical and Engineering Science*.

1025

DAVISON, A. C., PADOAN, S. A. & RIBATET, M. (2011). Statistical modelling of spatial extremes. *To appear in*
1026 *Statistical Science*.

1027

DE HAAN, L. (1984). A spectral representation for max-stable processes. *The Annals of Probability* **12**, 1194–1204.

1028

DE HAAN, L. & PEREIRA, T. T. (2006). *Spatial extremes: Models for the stationary case*. *The Annals of Statistics*
1029 **34**, 146–168.

1030

DE HAAN, L. & FERREIRA, A. (2006). *Extreme value theory: An introduction*. Springer Series in Operations Research
1031 and Financial Engineering.

1032

GENTON, M. G., MA, Y. & SANG, H. (2011). *On the likelihood function of Gaussian max-stable processes*.
1033 *Biometrika* **98**, 481–488.

1034

GENZ, A. (1992). Numerical computation of multivariate normal probabilities. *J. Comp. Graph Stat* **1**, 141–149.

1035

KABLUCHKO, Z., SCHLATHER, M. & DE HAAN, L. (2009). Stationary max-stable fields associated to negative
1036 definite functions. *Ann. Prob.* **37**, 2042–2065.

1037

KABLUCHKO, Z. & SCHLATHER, M. (2010). Ergodic properties of max-infinitely divisible processes. *Stochastic*
1038 *Processes and their Applications*, 120(3):281–295.

1039

1040

1041

- 1057 LIU, J., WONG, W. & KONG, A. (1995). Correlation structure and convergence rate of the Gibbs sampler with
1058 various scans. *Journal of the Royal Statistical Society Series B* **57**, 157–169.
- MANDELBROT, B. (1982). *The fractal geometry of nature*. W. H. Freeman.
- 1059 OESTING, M., KABLUCHKO, Z. & SCHLATHER, M. (2011). Simulation of Brown–Resnick processes. *To appear*
1060 *in Extremes*.
- 1061 PADOAN, S. A., RIBATET, M. & SISSON, S. (2010). Likelihood-based inference for max-stable processes. *Journal*
1062 *of the American Statistical Association* **105**, 263–277.
- 1063 R DEVELOPMENT CORE TEAM (2011). *R: A Language and Environment for Statistical Computing*. R Foundation
for Statistical Computing, Vienna, Austria. ISBN 3-900051-07-0.
- 1064 RIBATET, M. (2011). *SpatialExtremes: Modelling Spatial Extremes*. R package version 1.8-5.
- 1065 SCHLATHER, M. (2002). Models for stationary max-stable random fields. *Extremes* **5**, 33–44.
- 1066 SCHLATHER, M. (2011). *RandomFields: Simulation and Analysis of Random Fields*. R package version 2.0.53.
- 1067 SCHLATHER, M. & TAWN, J. (2003). A dependence measure for multivariate and spatial extremes: Properties and
inference. *Biometrika* **90**, 139–156.
- 1068 WANG, Y. (2010). *maxLinear: Conditional samplings for max-linear models*. R package version 1.0.
- 1069 WANG, Y. & STOEV, S. A. (2011). Conditional sampling for spectrally discrete max-stable random fields. *Advances*
in Applied Probability **43**, 461–483.

1070

1071

1072

1073

1074

1075

1076

1077

1078

1079

1080

1081

1082

1083